

Phase transformations of Al-bearing high-entropy alloys $\text{Al}_x\text{CoCrFeNi}$ ($x = 0, 0.1, 0.3, 0.75, 1.5$) at high pressure

Cite as: Appl. Phys. Lett. **114**, 091902 (2019); doi: [10.1063/1.5079868](https://doi.org/10.1063/1.5079868)

Submitted: 4 November 2018 · Accepted: 20 February 2019 ·

Published Online: 5 March 2019





View Online



Export Citation



CrossMark

Chenxu Wang,¹ Cameron L. Tracy,^{1,2}  Sulgiye Park,¹ Jin Liu,¹ Feng Ke,¹ Fuxiang Zhang,³ Tengfei Yang,⁴ Songqin Xia,⁵ Congyi Li,⁴ Yugang Wang,⁵ Yong Zhang,⁶  Wendy L. Mao,^{1,7} and Rodney C. Ewing^{1,a)}

AFFILIATIONS

¹Department of Geological Sciences, Stanford University, Stanford, California 94305, USA

²Belfer Center for Science and International Affairs, Kennedy School of Government, Harvard University, Cambridge, Massachusetts 02138, USA

³Division of Materials Science and Technology, Oak Ridge National Laboratory, Oak Ridge, Tennessee 37831, USA

⁴Department of Nuclear Engineering, University of Tennessee, Knoxville, Tennessee 37996, USA

⁵State Key Laboratory of Nuclear Physics and Technology, Center for Applied Physics and Technology, Peking University, Beijing 100871, China

⁶State Key Laboratory for Advanced Metals and Materials, University of Science and Technology Beijing, Beijing 100083, China

⁷Stanford Institute for Materials and Energy Sciences, SLAC National Accelerator Laboratory, Menlo Park, California 94025, USA

^{a)} Author to whom correspondence should be addressed: rewing1@stanford.edu

ABSTRACT

Pressure-induced structural modifications in high-entropy alloys with varying Al contents, $\text{Al}_x\text{CoCrFeNi}$ ($x = 0, 0.1, 0.3, 0.75, 1.5$), have been investigated at pressures up to ~ 50 GPa by synchrotron X-ray diffraction and, following depressurization, by transmission electron microscopy (TEM). In $\text{Al}_x\text{CoCrFeNi}$ compounds with $x \leq 0.3$, all of which exhibit an initial single-phase face-centered cubic (fcc) structure, proportionality between the Al content and the critical pressure for transformation to hexagonal close-packed (hcp) phases, distinguished by a distinct planar stacking sequence, is observed. This is attributed to the structural distortion arising from the large size of Al atoms relative to those of the other constituent elements, which results in an increase in the formation energy of stacking faults and a decrease in compressibility. High-resolution TEM results demonstrate variation of the stacking sequence from ABCABC, typical of fcc materials, to ABABAB, typical of hcp materials, in CoCrFeNi following high pressure. In $\text{Al}_{0.75}\text{CoCrFeNi}$, which exhibits an initial dual-phase structure [fcc and body-centered cubic (bcc)], the result again shows the formation of a (hcp) phase despite its higher Al content, suggesting that the bcc phase may be more amenable to pressure-induced phase modification than is the fcc phase, which is absent for lower Al contents. However, the trend of transformation inhibition by increasing the Al content is again observed, with $\text{Al}_{1.5}\text{CoCrFeNi}$ retaining its initial structure up to the highest pressure achieved. Determination of these compositional trends in the high-pressure phase response of these materials may enable the production of new phase mixtures with precisely tuned phase proportions and potentially desirable properties.

Published under license by AIP Publishing. <https://doi.org/10.1063/1.5079868>

High-entropy alloys (HEAs) are commonly defined as solid solutions of five (or more) principal elements in near-equiatomic concentrations.¹ Compared with conventional alloys, HEAs exhibit excellent properties, such as simultaneous strength and ductility, wear resistance, fatigue resistance, and thermal stability.² Due to these properties, HEAs have recently attracted a great deal of interest and have been considered as promising candidates for a variety of structural applications, such as radiation tolerant cladding for nuclear fuel,³

damage tolerant materials at cryogenic temperatures,⁴ and soft magnetic materials.⁵

Due to their multi-component solid solution structures, severe lattice distortion is typically present in HEAs, yet the majority of them adopt two simple structures: face-centered cubic (fcc), body-centered cubic (bcc), or a mixture of both. This is attributed to the high configurational entropy, which is believed to stabilize the random solid solution structure. To design alloys with ideal properties for specific

applications, there is interest in processing methods that can expand this constrained HEA phase space. One strategy for creating new phases of HEAs is employing extreme environments (i.e., pressure, irradiation, temperature, etc.) to tune materials' structures and therefore their properties. For example, Tracy *et al.*⁶ observed a pressure-induced, partially irreversible transformation to a hexagonal close-packed (hcp) phase in the fcc transition metal alloy CoCrFeMnNi, one of the first HEAs observed. Additionally, Zhang *et al.*⁷ found that temperature influenced the critical pressure for the transformation. This allows for tuning the phase ratio of the fcc-hcp mixture without changing the HEA composition. Similar phase transformations have been reported in other Ni-based HEAs.⁸

Another common strategy in alloy development involves tailoring materials' properties by tuning the specific composition of a material. For example, the structure and mechanical properties of Al-bearing HEAs, $\text{Al}_x\text{CoCrFeNi}$ ($0 \leq x \leq 2$), vary dramatically with x , the Al content. These Al-bearing HEAs adopt fcc structures with $x \leq 0.5$, fcc + B2 (ordered bcc) duplex structures with $0.5 < x < 0.9$, and bcc (disordered) + B2 (ordered bcc) structures with $x > 0.9$.⁹

Combination of extreme environment processing and compositional tuning might be a means of further expanding the phase space of useful HEAs. Therefore, it is important to understand the role of the Al content in phase stability not only at ambient conditions but also at high pressure. Recently, an fcc structured Al-bearing HEA, $\text{Al}_{0.3}\text{CoCrFeNi}$, and a bcc structured Al-bearing HEA, $\text{Al}_2\text{CoCrFeNi}_2$, were reported to undergo no phase transformation up to a pressure of 60 GPa.¹⁰ However, the phase behaviors of various Al-bearing HEAs, as well as the mechanism of phase transformation in these HEAs at high pressure, have not been well studied.

Here, we report a study of the phase stabilities of a series of Al-bearing HEAs, $\text{Al}_x\text{CoCrFeNi}$ ($x = 0, 0.1, 0.3, 0.75, 1.5$), at pressures up to ~ 50 GPa using synchrotron X-ray diffraction (XRD) and transmission electron microscopy (TEM). Polycrystalline Al-bearing HEAs were

synthesized by arc melting under a Ti-gettered, high-purity Ar atmosphere and drop cast into water-cooled copper molds. Powder samples were obtained by scraping from the bulk samples using a diamond pen and were subsequently loaded, along with ruby pressure calibrants, into symmetric diamond anvil cells (DACs) with $300\text{ }\mu\text{m}$ diameter culets. Holes of $130\text{ }\mu\text{m}$ diameters were drilled in W gaskets to serve as sample chambers. Silicone oil was loaded into the chambers loaded as a pressure transmitting medium. High-pressure X-ray diffraction measurements were performed at beamline 16-BM-D of the Advanced Photon Source (APS), Argonne National Laboratory. A monochromatic X-ray beam ($\lambda = 0.4246\text{ }\text{\AA}$) was used for measurements of CoCrFeNi and a monochromatic X-ray beam ($\lambda = 0.4959\text{ }\text{\AA}$) was used for all other measurements. Two-dimensional diffraction patterns were recorded using a Mar345 detector and then integrated using the software Dioptas.¹¹ Unit cell parameters at each pressure step were determined from the index and the position of Bragg peaks using the software Unitcell.¹² Rietveld refinement was performed to determine quantitative phase fractions using the software GSAS-II.¹³ TEM samples were prepared by milling of the HEA samples, after quenching to ambient pressure and extraction from the DACs, using a focused ion beam system (FEI Helios NanoLab 600i DualBeam FIB). A 200 kV Tecnai F20 TEM was employed to investigate the atomic structure of the recovered samples.

Figure 1 shows XRD patterns of $\text{Al}_x\text{CoCrFeNi}$ ($x = 0, 0.1, 0.3, 0.75, 1.5$) at pressures up to ~ 50 GPa. Initially, $\text{Al}_x\text{CoCrFeNi}$ ($x = 0, 0.1, 0.3$) adopt fcc structures. With increasing pressure, their diffraction maxima shift towards higher angles due to unit cell compression. At ~ 14 GPa, there appear new diffraction maxima in CoCrFeNi, which are assigned to the (100) and (101) peaks of an hcp phase, as shown in Fig. 1(a). As the pressure is further increased, diffraction peaks corresponding to the initial fcc phase are attenuated, while the intensity of those corresponding to the hcp phase increases. However, at the highest pressure achieved, ~ 39 GPa, the initial fcc phase and the hcp phase still coexist. This demonstrates a sluggish fcc-to-hcp phase

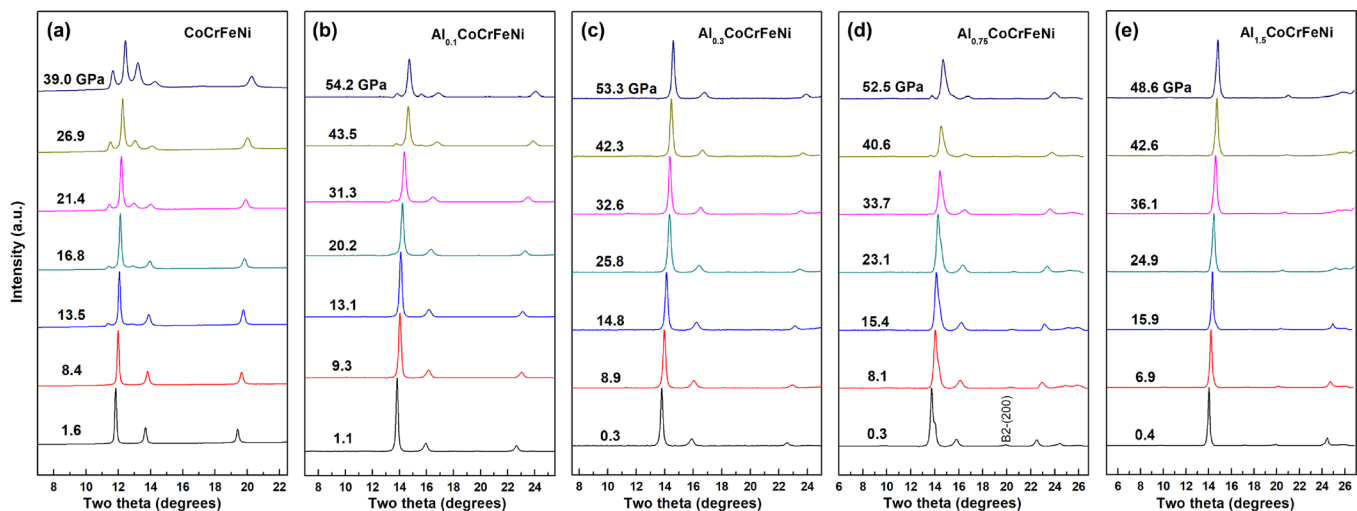


FIG. 1. X-ray diffraction patterns of Al-bearing HEAs: (a) CoCrFeNi, (b) $\text{Al}_{0.1}\text{CoCrFeNi}$, (c) $\text{Al}_{0.3}\text{CoCrFeNi}$, (d) $\text{Al}_{0.75}\text{CoCrFeNi}$, and (e) $\text{Al}_{1.5}\text{CoCrFeNi}$ at various pressures with a X-ray wavelength $\lambda = 0.4246\text{ }\text{\AA}$ (a) and $\lambda = 0.4959\text{ }\text{\AA}$ (b)–(e). Pressure triggers the formation of new diffraction peaks in CoCrFeNi, $\text{Al}_{0.1}\text{CoCrFeNi}$, and $\text{Al}_{0.75}\text{CoCrFeNi}$, starting at ~ 14 GPa, ~ 20 GPa, and ~ 34 GPa, respectively. No phase transformation was observed in $\text{Al}_{0.3}\text{CoCrFeNi}$ and $\text{Al}_{1.5}\text{CoCrFeNi}$. This indicates that the threshold pressure for the phase transformation increases with the Al content.

transformation, consistent with what was previously observed in CoCrFeMnNi at high pressure.^{6,7}

With the same initial fcc structure, Al_{0.1}CoCrFeNi and Al_{0.3}CoCrFeNi exhibit different responses to high pressure, as shown in Figs. 1(b) and 1(c), respectively. Similar fcc-to-hcp phase transformation is observed in Al_{0.1}CoCrFeNi. However, the critical pressure for this transformation increases to ~ 20 GPa, compared with ~ 14 GPa for CoCrFeNi. Additionally, only a small amount of hcp phase forms, with the majority of the material retaining its fcc phase even at the highest pressure achieved, ~ 54 GPa. In contrast, no phase transformation occurs in Al_{0.3}CoCrFeNi during the entire compression process, indicating that its fcc structure remains stable at high pressure. The hcp phase fractions in these three fcc-structured Al_xCoCrFeNi materials as a function of pressure as determined by Rietveld refinement are shown in Fig. 2. The slope of the hcp-CoCrFeNi phase fraction as a function of pressure is larger than that of hcp-Al_{0.1}CoCrFeNi, which is in turn larger than that of hcp-Al_{0.3}CoCrFeNi, indicating that the pressure-induced fcc-to-hcp phase transformation in Al_xCoCrFeNi is hindered by increasing the Al content. This is attributed to the fact that the size of the Al atoms in these alloys is significantly larger than that of other atoms.¹⁴ The higher the Al content, the larger the mean atomic size mismatch in the system. This leads to more lattice distortion in these materials at ambient pressure and subsequently increases the formation energy of stacking faults, which hinders the fcc-to-hcp transformation at high pressure. In our study, the fcc phases in CoCrFeNi and Al_{0.1}CoCrFeNi do not completely transform to the hcp phase at the highest pressures achieved; it is expected that the hcp fraction will continue to increase with pressure, as occurs in CoCrFeMnNi.⁶

During decompression back to ambient pressure, the pressure-induced hcp-CoCrFeNi phase is partially retained such that the quenched sample is a mixture of the residual fcc phase and the induced hcp phase. This is confirmed by high-resolution TEM (HRTEM) imaging of the quenched sample, as shown in Fig. 3(a). Two different stacking sequences, ABABAB and ABCABC, are observed, indicating that the fcc phase and hcp phase coexist after decompression. The

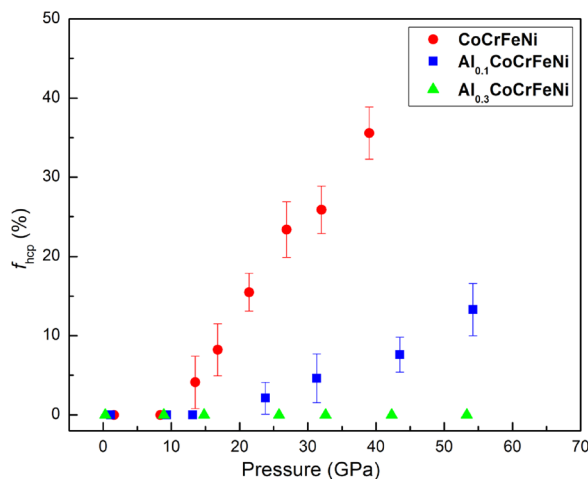


FIG. 2. The hcp phase fraction of Al_xCoCrFeNi ($x = 0, 0.1, 0.3$) as a function of pressure. The decreasing slope as a function of Al content indicates that the addition of this element hinders the fcc-to-hcp transformation.

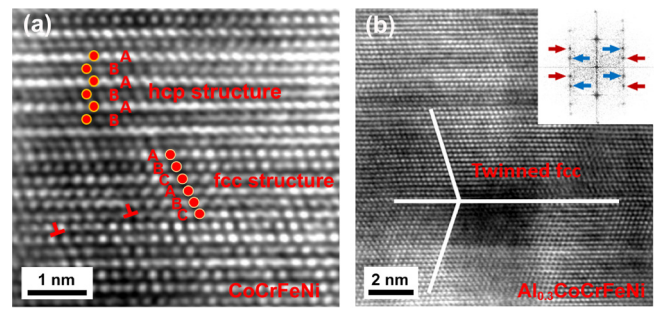


FIG. 3. HRTEM images of (a) CoCrFeNi and (b) Al_{0.3}CoCrFeNi samples after quenching to ambient pressure from ~ 39 GPa to ~ 53 GPa, respectively. A mixture of fcc and hcp phases is evident in CoCrFeNi. A pressure-induced nano-twinned fcc structure forms in Al_{0.3}CoCrFeNi, which is confirmed by the two set of diffraction spots indicated by the red and blue arrows in the inset fast Fourier transform (FFT).

mechanism of the fcc-to-hcp phase transformation is explained by the introduction of stacking faults along the close-packed planes, i.e., (111) in the fcc phase and (0001) in the hcp phase. The formation of stacking faults is attributed to the low stacking fault energy of these materials⁸ and was previously observed in similar HEAs during deformation.¹⁵ The phase ratio in this mixture of the fcc phase and the hcp phase can be tuned by controlling the maximum pressure achieved prior to quenching, allowing for tailoring of the material's properties (e.g., balancing of ductility and hardness). However, besides stacking faults, high concentrations of dislocations are observed, as indicated in Fig. 3(a). These features may also play a role in the observed transformation, although this requires further study.

The XRD results demonstrate that Al_{0.3}CoCrFeNi is structurally stable and retains its initial fcc structure up to ~ 53 GPa. However, in the HRTEM image of the quenched Al_{0.3}CoCrFeNi sample [Fig. 3(b)], a newly formed nano-twinned fcc structure is apparent, which was not observed in the initial material and could not be detected by the XRD experiment. This nano-twinned structure was also found in other HEAs following the application of strain^{4,16} and has been proposed as a source of high toughness¹⁷ and radiation tolerance.¹⁸ Therefore, high pressure processing provides a method for producing nano-twinned fcc structures with high densities of twin boundaries, which might be desirable in certain applications such as structural materials in nuclear energy systems, which demand high radiation tolerance. It should be noted that the intensity of the atomic columns in the hcp phase varies layer by layer. This might be attributed to certain types of atomic-ordering during the fcc-to-hcp phase transformation, such as Al segregation to certain planes.

Figures 4(a)–4(c) show the atomic volumes and unit cell parameters of Al_xCoCrFeNi ($x = 0, 0.1, 0.3$) as a function of pressure, as determined by the XRD measurement. Fitting of a third-order Birch-Murnaghan equation of state (EOS)¹⁹ to these data yields bulk moduli of $B_0 = 206(2)$ GPa with a pressure derivative $B'_0 = 4.2(2)$ for fcc-CoCrFeNi, $B_0 = 202(3)$ GPa with a pressure derivative $B'_0 = 4.8(2)$ for fcc-Al_{0.1}CoCrFeNi, and $B_0 = 193(3)$ GPa with a pressure derivative $B'_0 = 5.6(2)$ for fcc-Al_{0.3}CoCrFeNi, respectively, as shown in Table I. In addition, the atomic volumes of hcp-CoCrFeNi are fit well using the Birch-Murnaghan EOS, which yields a bulk modulus of $B_0 = 215(3)$ GPa with a pressure derivative $B'_0 = 4.2(2)$. These values obtained here are in good agreement with those calculated by density functional theory.²⁰

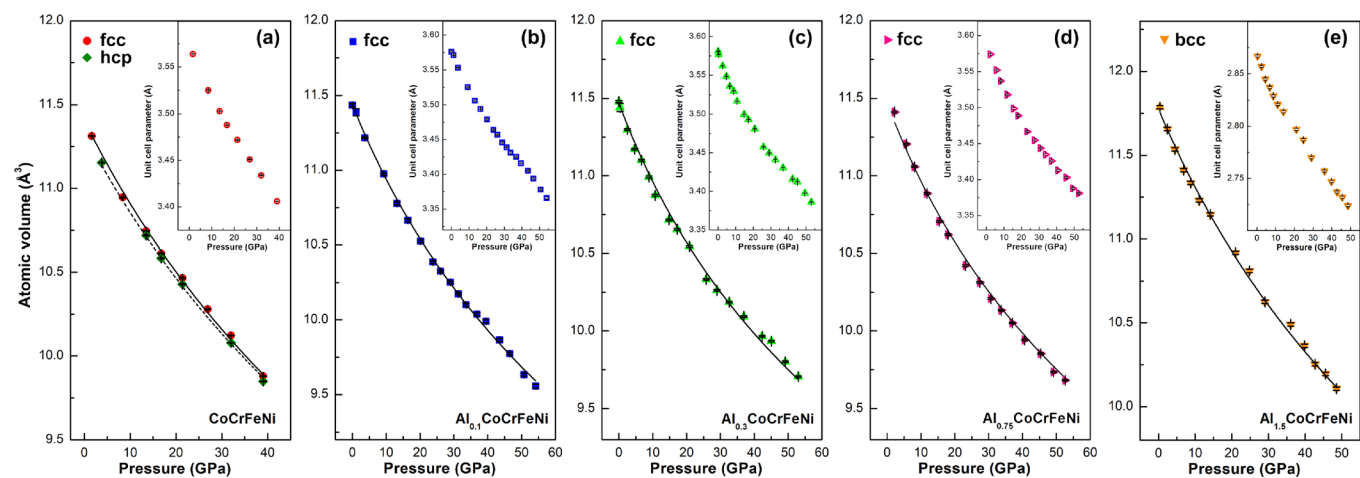


FIG. 4. Average atomic volumes and the corresponding unit cell parameters of fcc- $\text{Al}_x\text{CoCrFeNi}$ ($x = 0, 0.1, 0.3, 0.75$), hcp-CoCrFeNi, and bcc- $\text{Al}_{1.5}\text{CoCrFeNi}$ as a function of pressure. The lines illustrate the results of fitting of the P-V curves in all phases with the third order Birch-Murnaghan equation of state.

In contrast to those alloys with a lower Al content, $\text{Al}_{0.75}\text{CoCrFeNi}$ at ambient conditions adopts two phases: fcc and B2 (ordered bcc). Attenuation of this material's XRD peaks is also observed with increasing pressure. A new peak appears at $2\theta \approx 13.6^\circ$ starting at ~ 34 GPa, and a shoulder appears on the high 2θ side of the fcc-(111) peak at the highest pressure of ~ 53 GPa, indicating that a small amount of hcp phase is formed. Additionally, the peak at $\sim 19.8^\circ$, indexed as the (200) peak of the B2 phase,²¹ decreases in intensity as the pressure increases and disappears at a pressure of ~ 34 GPa. As mentioned above, in fcc-structured $\text{Al}_x\text{CoCrFeNi}$ systems, the critical pressure for the phase transformation increases with the Al content. Based on this compositional trend, pressure would not be expected to produce an fcc-to-hcp phase transformation in $\text{Al}_{0.75}\text{CoCrFeNi}$ at pressure below ~ 50 GPa. Therefore, these observations might suggest a phase transformation of the B2 phase to the hcp phase, which is caused by compression along [001] and shearing along [110] and which has been previously observed in other materials, such as iron. However, the phase ratio of the hcp phase is limited, even at the highest pressure of ~ 53 GPa. To better understand the mechanism of the phase transformation in $\text{Al}_{0.75}\text{CoCrFeNi}$, structural behavior at higher pressure will be further investigated.²² Fitting of the atomic volumes of the fcc phase in $\text{Al}_{0.75}\text{CoCrFeNi}$, as a function of pressure, with the third-order Birch-Murnaghan EOS yields a bulk modulus of $B_0 = 185(2)$ GPa with a pressure derivative $B'_0 = 5.6(2)$. Additionally, it should be noted that the atomic ratio of Ni in the fcc phase in $\text{Al}_{0.75}\text{CoCrFeNi}$ is only $\sim 17\%$, which is smaller than those of Co

(24%), Cr (26%), and Fe (26%).²¹ Compared to $\text{Al}_x\text{CoCrFeNi}$ ($x = 0, 0.1, 0.3$) with equiatomic concentrations of Co, Cr, Fe, and Ni, the structural response of the fcc phase in $\text{Al}_{0.75}\text{CoCrFeNi}$ to compression may be influenced not only by the Al compositional trend but also by the Ni-depleted environment in the material.

$\text{Al}_{1.5}\text{CoCrFeNi}$ is also a dual-phase HEA, containing the bcc phase and the B2 phase. No evident phase transformation is observed in our study, as shown in Fig. 1(e). Because bcc and related structures possess lower packing density than fcc structures and hcp structures, high pressure is usually expected to trigger the formation of phases with a denser structure. Surprisingly, bcc- $\text{Al}_{1.5}\text{CoCrFeNi}$ is stable during the entire compression range. This is consistent with the trend observed in the other Al-bearing HEAs: higher Al concentrations increase the stacking fault energy and therefore inhibit the phase transformation under high pressure. The bulk modulus of the bcc phase of this material, obtained by the fitting of the third-order Birch-Murnaghan EOS to the XRD results, is $B_0 = 226(2)$ GPa with a pressure derivative $B'_0 = 4.6(2)$. This bulk modulus is much higher than that predicted computationally (170 GPa).²⁰ This is likely due to the fact that this bcc phase is not near-equiatomic, due to compositional segregation between it and the accompanying B2 phase. The ratios of Al, Co, Cr, Fe, and Ni atoms are $\sim 5\%$, 9% , 53% , 32% , and 1% in the bcc phase, such that it is highly enriched in Fe and Cr, making it similar to an Fe-Cr alloy with the previously measured bulk modulus of $\sim 225(8)$ GPa.²³ Therefore, the structural stability under high pressure and the mechanical properties of $\text{Al}_{1.5}\text{CoCrFeNi}$ are not comparable

TABLE I. Bulk moduli and the corresponding pressure derivative of fcc-structured $\text{Al}_x\text{CoCrFeNi}$ ($x = 0, 0.1, 0.3, 0.75$) and bcc- $\text{Al}_{1.5}\text{CoCrFeNi}$. Note that the fcc phases in $\text{Al}_{0.75}\text{CoCrFeNi}$ and $\text{Al}_{1.5}\text{CoCrFeNi}$ are not equiatomic.

Compound	CoCrFeNi		$\text{Al}_{0.1}\text{CoCrFeNi}$	$\text{Al}_{0.3}\text{CoCrFeNi}$	$\text{Al}_{0.75}\text{CoCrFeNi}$		$\text{Al}_{1.5}\text{CoCrFeNi}$	
Phase	fcc	hcp	fcc	fcc	fcc	B2	bcc	B2
Bulk modulus (GPa)	206 (2)	215 (3)	202 (3)	193 (3)	185 (2)	...	226 (2)	...
Pressure derivative	4.2 (2)	4.2 (2)	4.8 (2)	5.6 (2)	5.6 (2)	...	4.6 (2)	...

with those of the other Al-bearing HEAs. The bulk moduli of the B2 phases in $\text{Al}_{0.75}\text{CoCrFeNi}$ and $\text{Al}_{1.5}\text{CoCrFeNi}$ were not fitted due to weak intensity of their super-lattice diffraction maxima.

In summary, the structural response of Al-bearing HEAs $\text{Al}_x\text{CoCrFeNi}$ ($x=0, 0.1, 0.3, 0.75, 1.5$) to high pressure was studied using synchrotron radiation XRD and HRTEM. A sluggish, pressure-induced transformation from the initial fcc phase to an hcp phase was observed in CoCrFeNi, starting at ~ 14 GPa. The critical pressure for this fcc-to-hcp phase transformation increases with the Al content in all Al-bearing HEAs $\text{Al}_x\text{CoCrFeNi}$ ($x=0, 0.1, 0.3$) due to the atomic size of the Al atoms in these alloys. A newly formed nano-twinned fcc structure in the recovered $\text{Al}_{0.3}\text{CoCrFeNi}$ was observed using TEM, providing additional insight into the local atomic processes driving the pressure-induced transformation, which could not be obtained from the *in situ* XRD measurements alone. In $\text{Al}_{0.75}\text{CoCrFeNi}$, a phase transformation to the hcp structure starts at ~ 34 GPa, as indicated by the disappearance of the B2 phase's diffraction maxima. The bcc- $\text{Al}_{1.5}\text{CoCrFeNi}$ phase is retained up to the highest studied pressure of ~ 49 GPa. These findings elucidate compositional trends in the high-pressure phase behavior of Al-bearing HEAs, demonstrating a means of producing alloys with various structures and mixtures of structures by simultaneous tuning of the composition and extreme environment processing conditions.

This work was financially supported by the National Magnetic Confinement Fusion Energy Research Project of China (2015GB113000) and the National Natural Science Foundation of China (11675005, 51471025, 51671020). Portions of this work were performed at HPCAT (Sector 16), Advanced Photon Source (APS), Argonne National Laboratory. HPCAT operations are supported by DOE-NNSA under Award No. DE-NA0001974 and DOE-BES under Award No. DE-FG02-99ER45775, with partial instrumentation funding by NSF. The Advanced Photon Source is a U.S. Department of Energy (DOE) Office of Science User Facility operated for the DOE Office of Science by Argonne National Laboratory under Contract No. DE-AC02-06CH11357. The HPCAT beamtime was supported and allocated by the Carnegie/DOE Alliance Center (CDAC) under DOE-BES Award No. DE-NA0002006. Part of this work was performed at the Stanford Nano Shared Facilities (SNSF), supported by the National Science Foundation under Award No. ECCS-1542152.

REFERENCES

- ¹B. Cantor, I. T. H. Chang, P. Knight, and A. J. B. Vincent, *Mater. Sci. Eng. A* **375**, 213 (2004); Y. Zhang, T. T. Zuo, Z. Tang, M. C. Gao, K. A. Dahmen, P. K. Liaw, and Z. P. Lu, *Prog. Mater. Sci.* **61**, 1 (2014); J. W. Yeh, S. K. Chen, S. J. Lin, J. Y. Gan, T. S. Chin, T. T. Shun, C. H. Tsau, and S. Y. Chang, *Adv. Eng. Mater.* **6**(5), 299 (2004).
- ²M. S. Lucas, G. B. Wilks, L. Mauger, J. A. Munoz, O. N. Senkov, E. Michel, J. Horwath, S. L. Semiatin, M. B. Stone, and D. L. Abernathy, *Appl. Phys. Lett.* **100**(25), 251907 (2012); J.-W. Yeh, *JOM* **65**(12), 1759 (2013); Z. Li, K. G. Pradeep, Y. Deng, D. Raabe, and C. C. Tasan, *Nature* **534**(7606), 227 (2016).
- ³C. Lu, L. Niu, N. Chen, K. Jin, T. Yang, P. Xiu, Y. Zhang, F. Gao, H. Bei, S. Shi, M. R. He, I. M. Robertson, W. J. Weber, and L. Wang, *Nat. Commun.* **7**, 13564 (2016); Y. Zhang, G. M. Stocks, K. Jin, C. Lu, H. Bei, B. C. Sales, L. Wang, L. K. Beland, R. E. Stoller, G. D. Samolyuk, M. Caro, A. Caro, and W. J. Weber, *ibid.* **6**, 8736 (2015).
- ⁴B. Gludovatz, A. Hohenwarter, D. Catoor, E. H. Chang, E. P. George, and R. O. Ritchie, *Science* **345**(6201), 1153 (2014).
- ⁵Y. Zhang, T. Zuo, Y. Cheng, and P. K. Liaw, *Sci. Rep.* **3**, 1455 (2013).
- ⁶C. L. Tracy, S. Park, D. R. Rittman, S. J. Zinkle, H. Bei, M. Lang, R. C. Ewing, and W. L. Mao, *Nat. Commun.* **8**, 15634 (2017).
- ⁷F. Zhang, Y. Wu, H. Lou, Z. Zeng, V. B. Prakapenka, E. Greenberg, Y. Ren, J. Yan, J. S. Okasinski, X. Liu, Y. Liu, Q. Zeng, and Z. Lu, *Nat. Commun.* **8**, 15687 (2017).
- ⁸F. X. Zhang, S. Zhao, K. Jin, H. Bei, D. Popov, C. Park, J. C. Neufeind, W. J. Weber, and Y. Zhang, *Appl. Phys. Lett.* **110**(1), 011902 (2017).
- ⁹W.-R. Wang, W.-L. Wang, and J.-W. Yeh, *J. Alloys Compd.* **589**, 143 (2014).
- ¹⁰K. V. Yusenko, S. Riva, W. A. Crichton, K. Spector, E. Bykova, A. Pakhomova, A. Tudball, I. Kupaenko, A. Rohrbach, S. Klemme, F. Mazzali, S. Margadonna, N. P. Lavery, and S. G. R. Brown, *J. Alloys Compd.* **738**, 491 (2018).
- ¹¹C. Prescher and V. B. Prakapenka, *High Pressure Res.* **35**(3), 223 (2015).
- ¹²T. J. B. Holland and S. A. T. Redfern, *Mineral. Mag.* **61**(1), 65 (1997).
- ¹³B. H. Toby and R. B. Von Dreele, *J. Appl. Crystallogr.* **46**(2), 544 (2013).
- ¹⁴S. Guo, C. Ng, J. Lu, and C. T. Liu, *J. Appl. Phys.* **109**(10), 103505 (2011).
- ¹⁵S. Huang, H. Huang, W. Li, D. Kim, S. Lu, X. Li, E. Holmstrom, S. K. Kwon, and L. Vitos, *Nat. Commun.* **9**(1), 2381 (2018).
- ¹⁶Z. Zhang, H. Sheng, Z. Wang, B. Gludovatz, Z. Zhang, E. P. George, Q. Yu, S. X. Mao, and R. O. Ritchie, *Nat. Commun.* **8**, 14390 (2017).
- ¹⁷X. Li, Y. Wei, L. Lu, K. Lu, and H. Gao, *Nature* **464**(7290), 877 (2010).
- ¹⁸X.-M. Bai, A. F. Voter, R. G. Hoagland, M. Nastasi, and B. P. Uberuaga, *Science* **327**(5973), 1631 (2010).
- ¹⁹F. Birch, *J. Appl. Phys.* **9**(4), 279 (1938).
- ²⁰T. Fuyang, D. Lorand, C. Nanxian, L. K. Varga, J. Shen, and V. Levente, *Phys. Rev. B* **88**(8), 085128 (2013).
- ²¹T. Yang, S. Xia, S. Liu, C. Wang, S. Liu, Y. Zhang, J. Xue, S. Yan, and Y. Wang, *Mater. Sci. Eng.: A* **648**, 15 (2015).
- ²²W. A. Bassett and E. Huang, *Science* **238**(4828), 780 (1987); B. Yaakobi, T. R. Boehly, D. D. Meyerhofer, T. J. Collins, B. A. Remington, P. G. Allen, S. M. Pollaine, H. E. Lorenzana, and J. H. Eggert, *Phys. Rev. Lett.* **95**(7), 075501 (2005).
- ²³P. Olsson, I. A. Abrikosov, L. Vitos, and J. Wallenius, *J. Nucl. Mater.* **321**(1), 84 (2003).